ANALYTICAL CALCULATION OF THERMOACOUSTIC MAGNETOHYDRODYNAMIC GENERATOR

MIRHOSEINI[1] T., ALEMANY[2] A.
[1] KU Leuven, Department of Electrical Engineering ELECTA/ESAT, Belgium
[2]SIMAP/EPM, CNRS UMR 5266, 1340 rue de la piscine, 38402 ST Martin d'Hères, France
E-mail address of corresponding author: seyed.mirhoseini@esat.kuleuven.be

Abstract: This paper is devoted to the analytical investigation of a pulsating MHD flow in a cylindrical channel, submitted to an applied DC magnetic field and an imposed harmonically oscillating thermo-acoustically generated pressure gradient. Produced electrical current is extracted by induction coil in connection with compensation capacitor placed around the MHD channel. The effect of conducting wall is also taken into account. The generator is analytically modeled by solving the system of induction and Navier-Stokes equations simultaneously. Sensitivity analysis of efficiency, output power and different power losses versus MHD non-dimensional numbers are presented.

1. Introduction

Most of the magnetohydrodynamic devices make use of the fact that orthogonal electric and magnetic fields in a conducting medium will produce a Lorentz force and thus a particle velocity in the third orthogonal direction. This principle is based on the concept of devices such as electromagnetic pumps and propulsion systems [1]. The pumps transform electromagnetic energy into mechanical energy the reverse transfer occurs in acoustic MHD generators [2]. On the other hand, in the acoustic MHD devices the electromagnetic force and consequently the fluid flow are oscillatory [1, 3]. The schematic of the Thermoacoustic-MHD system is demonstrated in figure 1, where the MHD generator is submitted to thermo acoustic oscillatory pressure forces. Based on how to extract the produced electrical power from the generator, two types of machines can be considered:

- conduction machines, which produce strong electric currents at low voltage and require electrodes to collect the produced current, which may be a handicap for questions of water tightness, and,
- induction machines, that produce electric current with adjustable strength and voltage and do not require any electrodes [2], [4], [5].

This paper presents the results of the investigation of the MHD generator coupled with thermo acoustic engine. The liquid metal oscillates horizontally in the cylindrical MHD channel, under the effect of the oscillatory pressure difference due to the thermo acoustic engine. The magnet placed around the channel, produces a radial constant magnetic field. The interaction between this magnetic field and the liquid motion induce an AC current in the fluid, and AC induced magnetic field which producing AC current in the coil connected with the load. The system is depicted in figure 2.

2. Description of the model.

The main elements of the model are given in figure 2. The active part of the generator with the length l supposed to be larger than the MHD channel depth g , so that it could be considered as infinitely long. MHD channel contains a liquid metal with the density ρ , dynamic viscosity μ , relative magnetic permeability μ_f and electrical conductivity σ_f . The oscillatory pressure gradient applied by the thermo acoustic engine with the amplitude $\frac{\nabla p}{l}$ causes a velocity field with the value $u_0\hat{x}$ and a pulsation ω in the liquid metal. This velocity field is radially submitted to a constant magnetic field $B = -B_0\hat{r}$. The interaction will be resulted in an AC induced current $j\hat{\varphi}$ and an AC induced magnetic field $b\hat{x}$ producing an AC current i in the coil windings. Magnetic flux closes its path through the core and the yoke with relative permeability μ_i and μ_e, respectively. The coil has N turns and is connected in series with the load circuit, including a correction capacitor C_{Load} and a resistive load R_{Load}. The effect of the conducting wall on the power loss of the generator is also taken into account by placing a very thin metal layer with electrical conductivity σ_w in contact with the liquid metal. The main notations of the generator are listed in Table 1.

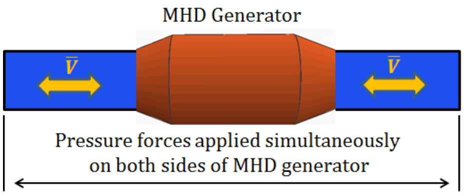

Figure 1. Schematic of the thermoacoustic MHD generator.

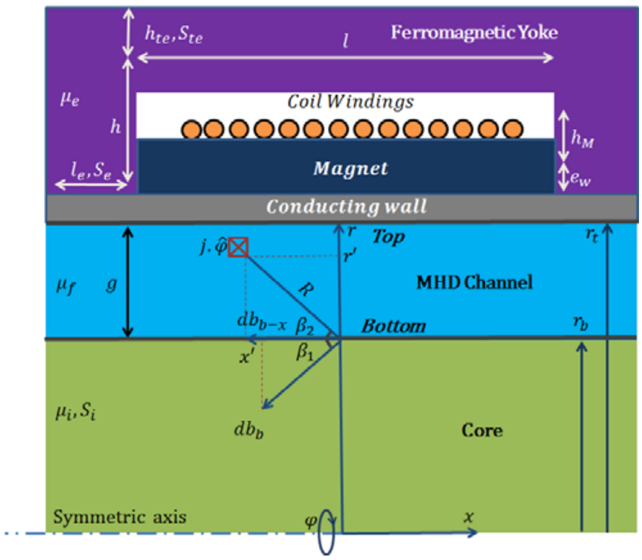

Figure 2. Schematic of the analytical model of the MHD generator, containing the core, MHD channel, ferromagnetic yoke, magnet and the induction coil.

3. Formulation of the problem

Governing equations are based on the following two sets:

a) Navier-Stokes equation which relates the velocity and the pressure with the Lorentz force
b) induction equation, which is a combination of Maxwell equations and Ohm's law.

Two main approximations are considered in the calculations. Due to the long channel aspect of the system ($l \gg g$) and the symmetry in the φ direction, we have:

Table 1. Scales of the MHD generator

Scales	Explanation
r_b	inner radius of the MHD channel
r_t	outer radius of the MHD channel
g	channel gap
e_w	wall thickness
h_M	magnet thickness
h	inner height of the yoke
h_{te}	thickness of the yoke
L_B	length of the active part
l_e	length of the yoke pole
S_i	cross section of the core
S_{te}	cross section of the yoke
S_e	cross section of the yoke leg

$$\frac{\partial}{\partial\varphi},\frac{\partial}{\partial x} \approx 0 \tag{1}$$

Moreover, since the depth of the channel is assumed to be several times smaller than the radius of the channel ($g \ll r_t, r_b$), the variations of the channel radius in the differential equation are approximated with the average radius of the channel:

$$r = r_{ch} = \frac{r_b + r_t}{2} \tag{2}$$

The non-dimensional system of differential equations to be solved is achieved as follows:

$$\begin{cases} iu^* = -K_p + \frac{1}{R_\omega}\left(\frac{\partial u^*}{r_{ch}\partial r^*}\right) + \frac{N}{R_m}\frac{\partial b^*}{\partial r^*} \\ ib^* = \frac{u^*}{r_{ch}} + \frac{u\partial^*}{\partial r^*} + \frac{1}{R_m}\frac{\partial b^*}{r_{ch}\partial r^*} + \frac{1}{R_m}\frac{\partial^2 b^*}{\partial r^{*2}} \end{cases} \tag{3}$$

where u^* , b^* and r^* are the non-dimensional values for fluid velocity, induced magnetic field density in the fluid and the depth of the channel, respectively. Also K_p , *N*, R_ω and R_m are the pressure factor, interaction parameter, Reynolds number and magnetic Reynolds number respectively.

The order 4 of the differential system in (3) shows that 4 boundary condition are needed to be determined to solve the system. Two of the boundary conditions are defined simply by the non-slip wall constrain:

$$u^*(r^* = r_b) = 0 \ , \ u^*(r^* = r_t) = 0 \tag{4}$$

Magnetic boundary condition includes the induced magnetic flux density at the bottom b_{bx} and at the top b_{bt} of the MHD channel. The magnetic flux density at the bottom of the channel in the *x* direction is a summation of the following three induced flux densities:

- b_{xf} = Magnetic flux density because of induced current inside the fluid
- b_{xw} = Magnetic flux density because of induced current inside the wall
- b_{xL} = Magnetic flux density because of current in the load

The load circuit configuration consists of a resistive load R_{Load} , correction capacitor C_{Load} and the induction coil with N_c number of turns. The current in the load circuit is proportional to the induced magnetic field at the bottom of the MHD channel via (5).

$$i^* = \frac{C_{Load}\mu_0 N_c S_i \omega^2}{g(1 + iR_{Load}C_{Load}\omega)} b^*_{bx} \tag{5}$$

The last boundary condition is the induced magnetic flux density at the top of the MHD channel which item could be achieved by applying the Ampere law once at the bottom and once at the top of the channel:

$$b_{tx}^{*} = \frac{1}{2}\left[\left(\frac{\mu_f}{\mu_t}\right)^2\left(2\frac{g}{L_B}\frac{\mu_i}{\mu_f}\frac{S_i}{S_e}+1\right)+1\right]b_{bx}^{*} \tag{6}$$

4. Results and Discussion

The system of differential equations (3) could be solved with the four boundary conditions mentioned in the previous section. The analytical expression for the u^* and b^* are very long, and are not presented in this paper for the sake of abbreviation. The results are presented in this section for the non-dimensional values of $R_m = 0.051$, $R_\omega = 32512$, $K_p = 6.22$, $N = 0.57$ and the load factor of $5.68\times10^{-4} - i3.51\times10^{-3}$. Figure 3(a) represents the velocity profile in the channel. The core of the channel has constant velocity amplitude, while in the boundary layer, a reverse flow is observed that is caused by the viscosity. This effect is also visible in Fig. 3(b), representing the current density evolution near the wall at the same time. The phase shift of the velocity profile changes the induced magnetic flux density pattern in the boundary layer. Since the fluid induced current density is proportional to the *r*-derivation of the induced magnetic flux density, j also is deformed in the boundary layer.

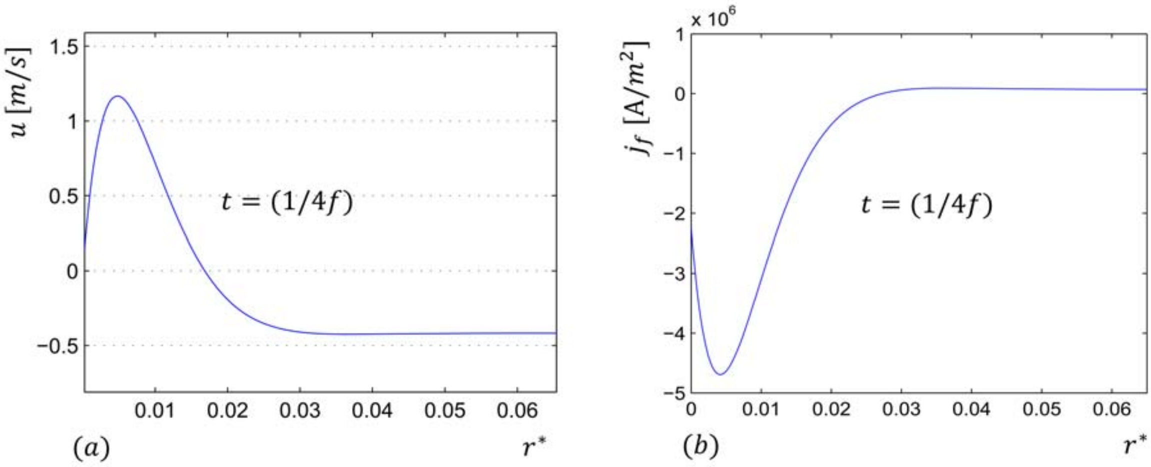

Figure 3. a) Velocity profile versus the channel depth at the time $t = 1/4f$, where a phase shif of velocity in the boundary layer is visible b) Induced current density profile versus the channel depth at the time $t = 1/4f$.

Efficiency behaviour as a function of magnetic Reynolds number and Reynolds number for fixed interaction parameter and different non-dimensional load resistances are demonstrated in figure 4 (a) and (b). It can be seen in Fig. 4(a) that for higher magnetic Reynolds number, the efficiency increases. That can be explained by the fact that by increasing the magnetic Reynolds number, the magnetic advection will dominate the magnetic diffusion in the fluid. This increases the effectiveness of the induction phenomenon and increases the induced current in the fluid and in the load. But by increasing the load resistance limits the current in the load circuit and will decrease the total output power. This enhances the efficiency of the system by making the fluid with better MHD qualities. The increase reaches saturation at higher values of R_m.

Figures 4(b) depicts the variations of the efficiency versus Reynolds number for four different non-dimensional load resistances and the constant interaction parameter and magnetic Reynolds number. This is a result of the fact that when increasing the frequency (R increases) the induced magnetic field does not penetrates in the conducting liquid and so the extracted power tends to zero as well as the efficiency.

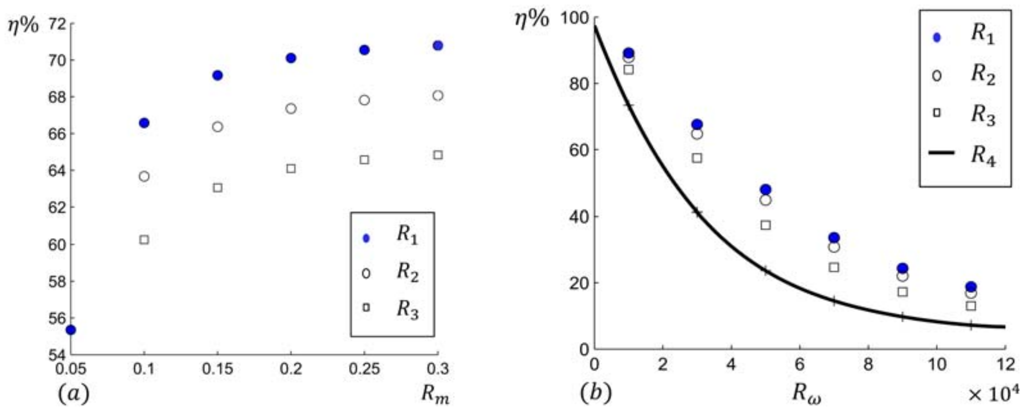

Figure 4. The efficiency versus a) magnetic Reynolds number and b) Reynolds number for different values of non-dimensional load resistances:
$R_1 = 4.57 \times 10^6$, $R_2 = 5.78 \times 10^6$, $R_3 = 9 \times 10^6$ and $R_4 = 1.98 \times 10^7$, with $N = 0.57$ and $R_m = 0.03$

5. Conclusion

This paper is about an analytical approach to study MHD generator which is in connection with a thermo acoustic engine that applies a fluid oscillation in the MHD channel. The analytical model is based on a system of differential equations, containing Navier-Stokes equation and the induction equation. The dimensionless differential equations are given exhibiting non-dimensional parameters. The solution of the system is achieved by applying the velocity and the induced magnetic field boundary conditions. The results of the different parameters and the sensitivity analysis of the system are presented for a specific situation.

6. References

[1] Castrejn-Pita, A. A.; Huelsz, G.: Heat-to-electricity thermoacoustic-magnetohydrodynamic conversion. Applied Physics Letters. 90, 174110 (2007).

[2] Alemany, A.; Krauze, A.: Al Radi, M.: Thermo acoustic - MHD electrical Generator. Energy Procedia, Vol. 6, 2011, 92100.

[3] Schreppl, S. C..; Busch-Vishni, I. J.: A magnetohydrodynamic underwater acoustic transducer. J. Acoust. Soc. Am., 89 (2), February 1991.

[4] Satyamurthy, P..; Venkatramani, N.: Quraishi, A. M.: Mushtaq, A.: A magnetohydrodynamic underwater acoustic transducer. Basic design of a prototype liquid metal magnetohydrodynamic power generator for solar and waste heat. Energy Conversion and Management, Vol. 40, 1999, 913-935

[5] Dixit, N. S.; Thyiagarajan, T. K.: Venkartramani, N.: Experimental study on the effect of insulating van and interaction parameter on current and voltage in a liquid metal MHD generator, J. Energy Conversion, Vol. 35, 1994, 643-649.